HHS Public Access

Author manuscript

Mol Cell. Author manuscript; available in PMC 2016 June 04.

Published in final edited form as:

Mol Cell. 2015 June 4; 58(5): 845–853. doi:10.1016/j.molcel.2015.04.015.

A Protein Kinase C phosphorylation motif in GLUT1 affects glucose transport and is mutated in GLUT1 deficiency syndrome

Eunice E. Lee[*,1], **Jing Ma**[*,1], **Anastasia Sacharidou**[2], **Wentao Mi**[3], **Valerie K. Salato**[4], **Nam Nguyen**[5], **Youxing Jiang**[5], **Juan M. Pascual**[2,3], **Paula E. North**[4], **Philip W. Shaul**[2], **Marcel Mettlen**[6], and **Richard C. Wang**[1]

[1]Department of Dermatology, UT Southwestern Medical Center, Dallas, TX, 75390

[2]Department of Pediatrics, UT Southwestern Medical Center, Dallas, TX, 75390

[3]Department of Neurology & Neurotherapeutics, UT Southwestern Medical Center, Dallas, TX, 75390

[4]Department of Pathology, Medical College of Wisconsin, Milwaukee, WI, 53226

[5]Department of Physiology, UT Southwestern Medical Center, Dallas, TX, 75390

[6]Department of Cell Biology, UT Southwestern Medical Center, Dallas, TX 75390

Summary

Protein Kinase C has been implicated in the phosphorylation of the erythrocyte/brain glucose transporter, GLUT1, without a clear understanding of the site(s) of phosphorylation and the possible effects on glucose transport. Through in-vitro kinase assays, mass spectrometry, and phosphospecific antibodies, we identify Serine 226 in GLUT1 as a PKC phosphorylation site. Phosphorylation of S226 is required for the rapid increase in glucose uptake and enhanced cell surface localization of GLUT1 induced by the phorbol ester 12-O-tetradecanoyl-phorbol-13-acetate (TPA). Endogenous GLUT1 is phosphorylated on S226 in primary endothelial cells in response to TPA or VEGF. Several naturally-occurring, pathogenic mutations that cause GLUT1 deficiency syndrome disrupt this PKC phosphomotif, impair the phosphorylation of S226 *in vitro*, and block TPA-mediated increases in glucose uptake. We demonstrate that the phosphorylation of GLUT1 on S226 regulates glucose transport and propose that this modification is important in the physiological regulation of glucose transport.

Corresponding author: Richard C. Wang, MD PhD, NL08.110FB, UT Southwestern Medical Center, 5323 Harry Hines Blvd, Dallas, TX 75390-9069, Office: 214-633-1860, Fax: 214-648-5554, richard.wang@utsouthwestern.edu.

Author Contributions

J.M. performed and analyzed experiments involving GLUT1 biochemistry and phosphorylation, including mass spectrometry. E.L. performed and analyzed glucose uptake studies, biotin labeling, and Xenopus oocyte experiments with assistance from R.W. W.M. performed oocyte injections with assistance from E.L. M.M. performed imaging experiments with assistance from R.W. A.S. and P.S. performed and analyzed most endothelial cell experiments with assistance from E.L. V.S. and P.N. performed and analyzed immunohistochemistry experiments. N.N. and Y.J. provided structural guidance and figures. J.P. enrolled volunteers and revised the manuscript. R.W. designed the project, analyzed experiments, and wrote the manuscript with contributions from E.L. and J.M.

*Equal contribution

Introduction

Tissues can rapidly modulate glucose transport in response to autonomous or extrinsic signals, but the mechanisms that regulate GLUT1 are still not completely understood. A rare pediatric neurological disease, GLUT1 deficiency syndrome (G1D), highlights the importance of precisely regulating glucose transport. A mutation in just one allele of *SLC2A1*, which encodes GLUT1, can cause movement disorders, epilepsy, and developmental delay (De Vivo et al.; Seidner et al.). The diversity and prevalence of neurological disease caused by *SLC2A1* mutations is greater than initially appreciated (Leen et al., 2010; Suls et al., 2009). Mutations that truncate or destabilize the *SLC2A1* transcript (e.g. nonsense, frame shift, splice junctions) often result in severe disease while missense mutants sometimes have more subtle clinical phenotypes (Leen et al., 2010). Even missense mutations that do not effect transporter expression or cell surface localization can cause neurological disease (Arsov et al., 2012; Wang et al., 2008). The phenotypic variability in the clinical presentation of G1D patients suggests nuances in the regulation of GLUT1-mediated glucose transport.

One of the first factors found to increase glucose uptake was the phorbol ester, 12-O-Tetradecanoylphorbol-13-acetate (TPA). Phorbol esters are extensively-characterized tumor promoters that exert pleiotropic effects on cell migration, proliferation, and survival through their actions on diacylglycerol (DAG)-dependent isoforms of Protein Kinase C (PKC) (Castagna et al., 1982). Phorbol esters induce a biphasic increase in glucose uptake, one with both rapid and slower components (Driedger and Blumberg). Transcriptional upregulation of GLUT1 explains the slow increase in glucose uptake that occurs in response to both TPA and viral oncogenes (Birnbaum et al., 1987; Flier et al., 1987). However, the early, transcription-independent increase in glucose uptake remains unexplained (Lee and Weinstein; O'Brien, 1982). While GLUT1 has been identified as a PKC substrate, the precise location(s) of modification and potential effects on GLUT1 were unclear (Deziel et al., 1989; Witters et al., 1985). We identify a serine phosphorylation site in GLUT1 that mediates the rapid, TPA-induced increases in glucose uptake. This phosphorylation occurs in endothelial cells and is impaired in rare cases of GLUT1 deficiency syndrome, suggesting that it plays a role in the physiological regulation of glucose uptake.

Results

Protein Kinase C isoforms phosphorylate GLUT1 *in vitro* and *in vivo*

Phorbol esters rapidly increase glucose uptake and activate DAG-dependent isoforms of PKC, so we tested whether PKC might phosphorylate GLUT1 *in vitro*. Previous studies localized a potential PKC site to its cytoplasmic domains (Deziel et al., 1989). GLUT1 has two large cytoplasmic domains—a ~65 amino acid loop (Loop6) after transmembrane helix 6 and a ~41 amino acid carboxy-terminal tail (Cterm) after transmembrane helix 12 (Hresko et al., 1994). Peptides corresponding to these regions of *R. norvegicus* GLUT1 were fused to a Glutathione S-transferase (GST) tag, purified from bacteria, and incubated with PKC isoforms. Both conventional and novel PKC isoforms (β1, γ, δ) could phosphorylate GST-Loop6, but not GST-Cterm (Fig. 1A). Alanine mutagenesis of evolutionarily conserved

serine and threonine residues in Loop6 revealed that PKC specifically phosphorylated GLUT1 on Serine 226 (S226) (Fig. S1A). Alignment of vertebrate homologs of GLUT1 reveals a highly conserved PKC motif surrounding S226 (Fig. 1B) that is not highly conserved in other facilitative glucose transporter isoforms (Fig. S1B). The location of basic (position −3, +3) and hydrophobic (position +1, +2) residues around S226 matches the consensus substrate sequences of several PKC isoforms (Nishikawa et al., 1997). A screen of 229 purified kinases confirmed that several PKC isoforms (δ, φ, and η) could phosphorylate the proposed peptide *in vitro* (Table S1). HeLa cell extracts could efficiently phosphorylate GST-Loop6 but not in the presence of the PKC inhibitor Gö-6983 (Fig. 1D). To assess GLUT1 phosphorylation *in vivo*, we analyzed the transporter by mass spectrometry. To facilitate purification, a hemagglutinin (HA) tag was inserted into the first extrafacial loop of GLUT1 between Ser55 and Ile56. Rat2 cells were transduced with HA-GLUT1, stimulated with TPA, and the GLUT1 transporter purified (Fig. S1C). Mass spectrometry revealed that GLUT1 is indeed phosphorylated on S226 (Fig. 1E). GLUT1 can alternate between inward and outward open conformations (Deng et al., 2014). Modeling of a phosphoserine onto S226 of GLUT1 confirmed that the site is on an intracellular helix of the central cytoplasmic loop with its sidechain exposed to the cytosol in both conformations (Fig. S2). Two custom phosphospecific antibodies against GLUT1 Phosphoserine 226 (pGLUT1 S226) were generated that specifically recognize *in vitro* phosphorylated GST-Loop6 peptides (Fig. S1D). Using these antibodies, PKCβ1 was found to phosphorylate full-length GLUT1 *in vitro*, but not when pretreated with a PKC inhibitor Gö-6983 (Fig. 1E). Serum starved Rat2 cells expressing untagged WT GLUT1 showed no detectable phosphorylation of GLUT1 on S226 while TPA-treated cells showed strong phosphorylation of the site (Fig. 1F). Endogenous GLUT1 protein was also phosphorylated after TPA treatment of Rat2 cells (Fig. S1E). Using phosphospecific antibody immunoprecipitation, we estimate that ~70-85% of GLUT1 is phosphorylated in TPA treated Rat2 cells (Miinea and Lienhard, 2003) (Fig S1F). Finally, the partial depletion of PKCα in HeLa cells impaired GLUT1 phosphorylation after TPA (Fig. S1G) implicating PKCα in GLUT1 phosphorylation in HeLa cells.

S226 phosphorylation is required for TPA-induced increases in glucose uptake

To assess the functional effects of GLUT1 phosphorylation, we first confirmed that Rat2 cells could rapidly increase glucose uptake in response to TPA. Fibroblasts treated with TPA for 30 minutes increased tritiated (^{3}H) 2-deoxyglucose (2-DG) uptake by ~50% in a dose responsive manner. This rapid induction of glucose uptake was inhibited by incubation with Gö-6983 suggesting that TPA exerted its effects through PKC (Fig. S3A). To assess if GLUT1 phosphorylation contributes to increased glucose uptake, wild type (WT) and Serine 226 to Alanine (S226A) mutant GLUT1 constructs were transduced into Rat2 cells. Both WT and mutant transporters were stably expressed ten-fold over the endogenous transporter (Fig. S3B). In the absence of TPA, 3-O-methyl-D-glucose (3-OMG) uptake (Fig. S3C), 2-DG uptake (Fig. 4E); endocytic trafficking assays (Fig. S3D, E), and cell proliferation (Fig. S3F) were not significantly different in cells expressing WT and 226A transporters. Serum starved Rat2 cells expressing WT GLUT1 showed minimal S226 phosphorylation while TPA-treated cells showed robust phosphorylation at that site (Fig. 2A). The weak signal in Rat2 S226A GLUT1 expressing cells is consistent with phosphorylation of the endogenous

GLUT1 transporter (Fig. S1E). Within 30 minutes of TPA treatment, Rat2 cells expressing WT GLUT1 dose dependently increase 2-DG glucose uptake by more than 50%. Strikingly, Rat2 cells expressing S226A GLUT1 did not increase glucose uptake in response to TPA (Fig. 2B). A time course experiment reveals that WT GLUT1 cells increased 2-DG uptake as early as 4 minutes after TPA treatment and that the response of WT GLUT1 was consistently greater than S226A cells (Fig. S3G). Because TPA might increase glucose uptake through indirect effects on glucose metabolism (i.e. hexokinase activation), the effect of GLUT1 S226 phosphorylation on the transport of the non-metabolizable 3-OMG was assessed. Replicate variability precluded analysis of 3-OMG uptake in mammalian cell culture, so *Xenopus* oocytes were used to determine the effects of S226 phosphorylation on the kinetics of glucose transport. Oocytes were injected with cRNA encoding either WT or S226A GLUT1, treated with TPA, and analyzed by Western blot and immunofluorescence. While both the WT and S226A transporters were expressed and localized to the cell membrane (Fig. 2C, D), pGLUT1 S226 could only be detected after TPA treatment in the membranes of WT, but not the S226A, expressing oocytes (Fig. 2C). Immunofluorescence confirmed a clear localization of pGLUT1 S226 at the cell membrane in WT, but not S226A expressing oocytes (Fig. 2D). 3-OMG uptake studies revealed that WT GLUT1 had a maximum uptake velocity (V_{max}) of ~385±81 pmol/oocyte/min and a Michaelis constant (K_m) of ~25.6±8.6mM. These values are consistent with previous analyses of the rat GLUT1 transporter in *Xenopus* oocytes (Nishimura et al., 1993). Treatment of the WT GLUT1 expressing oocytes with TPA markedly increased the V_{max} to ~879±134 and an increase of the K_m to ~50.1±14 mM. While the S226A transporter had similar transport kinetics as the WT transporter with a V_{max} of ~277±32 and K_m of ~23.8±5.8 mM, the mutant transporter was markedly less responsive to TPA and showed only a modest increase in its V_{max} to ~360±72 and K_m to ~31.4±8.7 mM after TPA treatment. In response to insulin, GLUT4 increases its V_{max} and by increasing transporters localization to the plasma membrane. We tested whether TPA might increase the localization of the GLUT1 to the plasma membrane using biotin to label and quantitate cell-surface GLUT1 abundance relative to a control plasma membrane protein (Na^+/K^+-ATPase) in Rat2 fibroblasts (Fig. 2F). Cell surface GLUT1 labeling was increased by 13.6% after treatment with TPA while pretreatment with Gö-6983 decreased GLUT1 cell surfacing labeling by 8.3% compared to untreated control cells (Fig. 2G). The presence of a small amount of HSP90, a cytosolic protein, in the membrane fraction suggests that the extent of GLUT1 localization to the cell surface induced by TPA may have been underestimated. We conclude that GLUT1 S226 phosphorylation increases glucose transport by increasing the V_{max} of GLUT1, at least in part through the increased cell surface localization of GLUT1.

GLUT1 S226 is phosphorylated in erythrocytes and endothelial cells

GLUT1 is expressed at high levels in erythrocytes, placenta, and blood-tissue barrier endothelial cells. It also functions as the basal glucose transporter for many tissues and is the most abundant isoform in proliferating endothelial cells, including umbilical vein and aortic endothelial cells (Mann et al., 2003). To address the physiological significance of GLUT1 S226 phosphorylation, primary erythrocytes and endothelial cells were analyzed. Erythrocytes from healthy donors showed increased pGLUT1 S226 in response to TPA (Fig. S4A). However, phosphorylation did not significantly change the rate of 3-OMG uptake in

erythrocytes (Fig. S4B). Treating primary human aortic endothelial cells (HAEC) with TPA resulted in increased pGLUT1 S226, which was abolished by pretreatment with Gö-6983 (Fig. 3A). TPA also induced a dose dependent increase in 2-DG uptake in endothelial cells, which was blocked by pretreatment with Gö-6983 (Fig. 3B, S6A). Several additional cell lines—HeLa, primary cardiac endothelial, EA.hy926, and b.End3 cells—demonstrated minimal pGLUT1 S226 after serum starvation or in the presence of 10% FBS, but showed clear phosphorylation when treated with TPA (Fig. S5A). Consistent with the modest effects of serum stimulation on GLUT1 phosphorylation, glucose uptake in serum-stimulated Rat2 cells was not affected by the expression of the S226A allele when compared to WT expressing cells (Fig. S5B).

The effect of TPA on GLUT1 and pGLUT1 localization in HUVEC was assessed. In serum-starved cells, total GLUT1 had a diffuse cytosolic localization. TPA stimulation increased overall GLUT1 staining, with a notable enrichment of signal at the cell membrane (Fig. 3C, top panel). While very little pGLUT1 S226 could be detected after serum-starvation, TPA stimulation strongly increased pGLUT1 staining, with a large proportion of the signal colocalizing with total GLUT1 at the plasma membrane in membrane ruffles (Fig. 3D, bottom panel). GLUT1 phosphorylation could also be detected in primary tissues *in situ*. Staining of acetone-fixed, frozen sections of lymphatic malformations showed a partial colocalization of pGLUT1 S226 and GLUT1 staining. Robust pGLUT1 S226 staining was noted in the perineurium and vascular smooth muscle (Fig. 3E).

We next assessed the effects of physiological levels of hormones on pGLUT1 S226. Vascular endothelial growth factor (VEGF) and Angiotensin II (AngII) induce rapid, transcription-independent increases in glucose uptake in endothelial and astroglial cells (Sone et al., 2000; Tang et al., 1995). Human umbilical vein endothelial cells (HUVEC) treated with VEGF (100ng/ml) or AngII (200nM) increased pGLUT1 S226 in a time-dependent manner (Fig. 3D, S6B). VEGF significantly increased pGLUT1 S226 within 15 minutes (Fig. 3E). VEGF induced similar changes in pGLUT1 S226 in primary human aortic endothelial cells (HAEC) (Fig. S6C, D). VEGF increased 2-DG uptake by more than 20%, an effect that was inhibited by pretreatment with Gö-6983 (Fig. 3F). Thus, primary endothelial cells phosphorylate GLUT1 on S226 and increase glucose uptake in response to phorbol esters and VEGF (Fig. 3D).

The GLUT1 S226 motif is mutated in cases of GLUT1 deficiency syndrome

Of the scores of pathogenic mutations in GLUT1 that have been identified (Leen et al., 2010), several reside in the PKC motif surrounding S226. Three missense mutants replace R223 with a non-conserved residue (P, Q, or W), and one splice-site mutation results in the in-frame insertion of three amino acids (PPV) between V227 and K228 (Arsov et al.; Leen et al.; Mullen et al.; Suls et al.). In each case, one or more residues critical for phosphorylation by PKC is replaced with a non-conserved amino acid (Nishikawa et al.) (Fig. 4A). We introduced these naturally-occurring mutations into the WT GLUT1 sequence. A G1D-associated mutation in Loop6 of GLUT1 (K256E), which is not predicted to affect the PKC motif at S226, was included as a control. GST fusion proteins with PKC motif mutations were expressed at similar levels as the WT protein but were not efficiently

phosphorylated by PKC *in vitro* (Fig. 4B). The loss of pGLUT1 S226 was not a general feature of mutant transporters as several G1D associated mutations (K256E, R333W, and T295M) were still efficiently expressed and phosphorylated compared to the WT GLUT1 transporter *in vivo* (Fig. 4C, data not shown). Each of the mutants could also be stably overexpressed in Rat2 cells (Fig. 4D). Despite the slightly lower abundance of the R223P, R223W, and 227insPPV mutants, all of the mutant GLUT1 transporters had similar levels of basal 2-DG uptake when compared to the WT transporter (Fig. 4E). While the K256E mutant maintained its ability to respond to TPA, all PKC motif mutations showed markedly decreased responsiveness (Fig. 4F, G). G1D mutations in phosphorylation motif surrounding S226 impair GLUT1 phosphorylation and response to TPA.

Discussion

PKC was first found to phosphorylate GLUT1 about 30 years ago (Witters et al., 1985). Later, it was found that insulin triggered glucose uptake through GLUT4, independent of GLUT1 phosphorylation (Gibbs et al., 1986), so interest in PKC-GLUT1 signaling diminished. However, because this phosphorylation is required for rapid increases in glucose transport, present in primary tissues, and impaired in G1D, we contend that GLUT1 S226 phosphorylation contributes significantly to the physiological regulation of glucose transport. Although our findings are specific for GLUT1, the phosphorylation of other facilitative glucose transporters might also contribute to their regulation.

Although humans possess eleven PKC isozymes, only the conventional and novel isoforms require DAG for signaling. As diverse, tissue-specific stimuli (e.g. hormones, neurotransmitters, and growth factors) can all activate PKC through heterotrimeric G_q protein and phospholipase C, pGLUT1 S226 may contribute to the rapid regulation of glucose uptake in many settings (Sone et al., 2000; Tang et al., 1995). The incomplete colocalization of pGLUT1 S226 and total GLUT1 suggests that tissues differ in the basal activation of GLUT1 by PKC. Moreover, as other kinases can phosphorylate GLUT1 S226 motif *in vitro*, there may be some settings in which S226 phosphorylation occurs independently of PKC. Ultimately, it will be important to determine how diverse, cell-specific stimuli are integrated with known GLUT1 signaling pathways (e.g. Akt, AMPK) to modulate transporter function *in vivo* (Barnes et al., 2002; Wieman et al., 2007).

TPA-stimulated phosphorylation of GLUT1 must increase glucose uptake by increasing the number of GLUT1 transporters in the plasma membrane and/or by increasing the activity of the transporter. Our analyses in *Xenopus* oocytes demonstrate that pGLUT1 S226 increases glucose uptake largely by increasing V_{max}. Consistent with these kinetic studies, TPA increased the localization of GLUT1 to the cell membrane as assessed by both biochemical and immunofluorescence assays in cell culture. Perhaps due to the absence of vesicle trafficking machinery, the phosphorylation of GLUT1 was not associated with an increase in glucose transport in erythrocytes. While recent structural models do not identify a direct role for S226 in GLUT1 transporter conformation (Deng et al., 2014), additional studies on isolated transporters are necessary to exclude effects of S226 phosphorylation on GLUT1 catalytic activity. Overall, our results support a model in which phosphorylation of the

glucose transporter by PKC increases glucose transport at least in part through an increased localization of the phosphorylated transporter to the plasma membrane.

While mutations of the motif surrounding S226 clearly impair its phosphorylation, the mutations may have additional effects on the transporter. For example, the R223 residue participates in hydrogen bond interactions that stabilize the transporter's inward open configuration (Deng et al., 2014), so mutations at this site might also alter the intrinsic properties of the transporter. Functional studies of specific mutations in *Xenopus* oocytes have revealed defects in the kinetic properties of the R223P mutant (Suls et al., 2009) (i.e. a decreased V_{max}) but not the R223Q mutant (Arsov et al., 2012). Our assays did not reveal significant basal impairments in 2-DG uptake by any of the GLUT1 mutants, including R223P. Regardless of the effects of these mutations on basal glucose transport, these mutations do have clear defects in phosphorylation and TPA-induced glucose transport, which may contribute to the functional defects seen in a subset of G1D patients.

Patients with S226 motif mutations develop symptoms despite the presence of one normal allele of *SLC2A1*, suggesting that such mutations may exert dominant negative effects. This clinical observation is consistent with the decreased response of cells expressing S226 motif mutants to TPA, despite the presence of endogenous GLUT1. Because the ketogenic diet, the most common treatment for G1D, is an imperfect treatment (Klepper and Leiendecker, 2013), additional treatment options would greatly benefit G1D patients. Whether vascular endothelial cells, blood-brain barrier cells, or other GLUT1-expressing tissues are to blame for the symptoms of G1D is currently unclear. Studies on the localization and function of pGLUT1 S226 in normal and G1D affected tissues will likely yield insights into the physiological regulation of GLUT1, which may in turn provide targetable pathways in the disease.

The upregulation of GLUT1 activity appears to be an important feature of many cancers. While many cancers increase glucose uptake through the increased expression of GLUT1 (Yamamoto et al., 1990; Younes et al., 1996), how signaling pathways regulate transporter activity and localization in these cancers is poorly understood. The loss-of-function mutations found in PKC in many cancers could affect GLUT1 S226 phosphorylation and membrane localization (Antal et al., 2015). Therefore, the analysis of GLUT1 transporter phosphorylation and localization in primary tissues *in situ* should yield insight into the regulation of the glucose transporters in health and disease.

Experimental Procedures

Cloning, Reagents, Cell Lines, and Antibodies

Details on cloning, reagents, cell lines, and antibodies are included in the supplemental information.

In vitro kinase assays

Assays were performed as described previously (Vergarajauregui et al., 2008). Briefly, GST proteins were incubated with recombinant human active PKC βI, PKC ζ (Life Technologies; P2291, P2273), PKC δ (R&D systems; 4585-KS), PKC γ (Sigma; P9542), or HeLa cell

extracts and [γ-^{32}P]ATP. Samples were stained with Coomassie Blue, dried, and subjected to autoradiography. For full-length GLUT1, lysates of serum-starved Rat2 HA-GLUT1 were immunoprecipitated with α–HA conjugated sepharose (CST, C29F4), eluted, and incubated with PKC. Reactions were stopped by the addition of sample buffer, and GLUT1 and pGLUT1 were detected by Western blot. Reactions were pretreated with 5μM Gö-6983 for 30 min if indicated.

Mass Spectrometry

HA-tagged proteins were immunoprecipitated from TPA treated Rat2 HA-GLUT1 or vector lysates. After washing, the sample was eluted with sample buffer for Coomassie Blue staining and Western Blotting (after dilution). The GLUT1 protein region was excised from a Coomassie stained gel and submitted for analysis by the UTSW Proteomics Core. The sample was trypsin digested; processed on a Q-Exactive mass spectrometry platform, using a short reverse-phase LC-MS/MS method; and analyzed using CPFP.

Determination of GLUT1 Phosphorylation Stoichiometry

Stoichiometry of pGLUT1 S226 was estimated as described previously (Miinea and Lienhard, 2003). Briefly, phosphorylated GLUT1 was immunoprecipitated from Rat2 GLUT1 lysates with pGLUT1 S226 (ThermoScientific). Serial dilutions of input and IP samples were analyzed by Western Blot for total GLUT1 antibody and pGLUT1 S226 (ThermoPierce). The ONE-HOUR Western Detection System (GenScript, L00241) prevented heavy chain interference. ImageJ was used to quantitate the band intensity and linear regression was used to calculate the relative IP efficiencies. The absolute IP efficiency using the pGLUT1 S226 antibody was ~0.24% (=47%/200) for total GLUT1 and ~0.34% (=67%/200) for phosphorylated GLUT1 due to the stringent IP conditions. The ratio of the total GLUT1 to pGLUT1 IP efficiency approximates the percentage of pGLUT1 S226.

Immunofluorescence and immunohistochemistry

For immunofluorescence, cells were plated on chamber slides (Lab-Tek), fixed in 4% paraformaldehyde, and permeabilized in 0.5% NP-40. Cells were stained with goat anti-GLUT1 (1:200; Santa Cruz) or anti-pGLUT1 S226 (1:200; Thermo) and secondary Alexa Fluor 488 or 546. Images were captured and figures prepared using identical acquisition and intensity settings (Edelstein et al., 2010). For immunohistochemistry, flash frozen lymphatic malformation tissue was fixed in acetone. The primary antibody was added [pGLUT1 (Thermo, 1:400) or GLUT1 (Labvision, 1:200)] followed by secondary antibody detection with MACH2 Universal HRP (Biocare Medical), visualization with DAB (Dako), and counterstaining with hematoxylin.

^{3}H-2-deoxyglucose (2-DG) transport assay

Cells were seeded in triplicate on 12-well plates (150-200,000 cells/well) for 18-24 hr, washed twice with PBS, and incubated in serum-free DMEM with 0.1% BSA for 2 hr. For dose response experiments, cells were treated with varying concentrations of TPA in KRH + 1mM pyruvate (KRHP) for 30 min. For time course experiments, cells were first preincubated in KRHP for 30 min prior to treatment with 250nM TPA for the indicated time

points. For serum refeeding experiments, cells were treated with 10% FBS for 20 min and washed twice with PBS. After treatment, uptake was initiated by adding 1μCi ^{3}H 2-DG and 0.1mM unlabeled 2-DG in KRHP to each well for 5 min. Control experiments showed that 2-DG uptake was linear during the 5 min time both with and without TPA (Fig. S3H). Transport was terminated by the rapid removal of uptake medium and washing with cold PBS with 25mM glucose. Cells were lysed with 0.5ml 0.5M NaOH, neutralized with 0.5ml 0.5M HCl, and quantitated by liquid scintillation counting. Protein concentrations were determined by BCA assay. Data were analyzed using GraphPad Prism.

Xenopus Assays

GLUT1 WT and S226A constructs were subcloned into a Xenopus expression vector, and their mRNA were synthesized in vitro. Oocytes (Ecocyte) were injected with 50ng of cRNA (1μg/μl) or water and incubated in ND96 medium for 72 hrs. [^{3}H]3-O-methylglucose (3-OMG) transport assays were performed as previously described with some modifications (Arsov et al., 2012; Weber et al., 2008). Oocytes were treated with 500nM TPA or DMSO for 20 min and uptake was initiated by adding 1.5μCi of [^{3}H]3-OMG (Perkin Elmer) and unlabeled 3-OMG (1 to 50mM). Transport proceeded for 4 min and was stopped by washing with ice-cold PBS with 0.2mM phloretin. Control experiments confirmed that 3-OMG uptake was linear during the 4 min incubation period (Fig. S3I). Oocytes were lysed in 1% SDS, and radioactivity was measured by liquid scintillation counting. Uptake was calculated by subtracting uptake by water-injected oocytes, which were assayed in parallel. Total membrane extracts were prepared from 10 injected oocytes and analyzed by Western blotting. For immunofluorescence, injected oocytes were fixed in 4% paraformaldehyde, permeabilized in methanol, sectioned, and stained as described above.

Determination of cell surface GLUT1

Biotinylation of Rat2 Cells was performed as described previously (Cura and Carruthers, 2010). Briefly, Rat2 cells were serum starved and treated with TPA for 30 min with pre-treatment by a PKC inhibitor if indicated. Cell surface proteins were labeled with EZ-Link Biotin (Thermo) in PBS for 30 min on ice followed by quenching. Supernatants containing the biotin labeled proteins (input) were immunoprecipitated with streptavidin beads (Thermo). The beads were washed and eluted with sample buffer. Na^{+}/K^{+}-ATPase was used as a membrane protein loading control. Band densities were quantified using Image Studio Lite (Licor).

Supplementary Material

Refer to Web version on PubMed Central for supplementary material.

Acknowledgements

We thank Gus Lienhard and Mike White for helpful discussions; Loderick Matthews for assistance with cryosectioning; Rosa Sirianni and Chieko Mineo for assistance with glucose uptake protocols; and Stephen Cannon for the use of microinjection equipment. This work was supported by NCI K08 (CA164047), Burroughs Wellcome Fund CAMS (1010978), American Cancer Society/Simmons Cancer Center (ACS-IRG-02-196), and Disease Oriented Clinical Scholar Awards to R.W.

References

Antal CE, Hudson AM, Kang E, Zanca C, Wirth C, Stephenson NL, Trotter EW, Gallegos LL, Miller CJ, Furnari FB, et al. Cancer-Associated Protein Kinase C Mutations Reveal Kinase's Role as Tumor Suppressor. Cell. 2015; 160:489–502. [PubMed: 25619690]

Arsov T, Mullen SA, Rogers S, Phillips AM, Lawrence KM, Damiano JA, Goldberg-Stern H, Afawi Z, Kivity S, Trager C, et al. Glucose transporter 1 deficiency in the idiopathic generalized epilepsies. Ann Neurol. 2012; 72:807–815. [PubMed: 23280796]

Barnes K, Ingram JC, Porras OH, Barros LF, Hudson ER, Fryer LG, Foufelle F, Carling D, Hardie DG, Baldwin SA. Activation of GLUT1 by metabolic and osmotic stress: potential involvement of AMP-activated protein kinase (AMPK). J Cell Sci. 2002; 115:2433–2442. [PubMed: 12006627]

Birnbaum MJ, Haspel HC, Rosen OM. Transformation of rat fibroblasts by FSV rapidly increases glucose transporter gene transcription. Science. 1987; 235:1495–1498. [PubMed: 3029870]

Castagna M, Takai Y, Kaibuchi K, Sano K, Kikkawa U, Nishizuka Y. Direct activation of calcium-activated, phospholipid-dependent protein kinase by tumor-promoting phorbol esters. J Biol Chem. 1982; 257:7847–7851. [PubMed: 7085651]

Cura AJ, Carruthers A. Acute modulation of sugar transport in brain capillary endothelial cell cultures during activation of the metabolic stress pathway. J Biol Chem. 2010; 285:15430–15439. [PubMed: 20231288]

De Vivo DC, Trifiletti RR, Jacobson RI, Ronen GM, Behmand RA, Harik SI. Defective glucose transport across the blood-brain barrier as a cause of persistent hypoglycorrhachia, seizures, and developmental delay. N Engl J Med. 1991; 325:703–709. [PubMed: 1714544]

Deng D, Xu C, Sun P, Wu J, Yan C, Hu M, Yan N. Crystal structure of the human glucose transporter GLUT1. Nature. 2014; 510:121–125. [PubMed: 24847886]

Deziel MR, Lippes HA, Rampal AL, Jung CY. Phosphorylation of the human erythrocyte glucose transporter by protein kinase C: localization of the site of in vivo and in vitro phosphorylation. The International journal of biochemistry. 1989; 21:807–814. [PubMed: 2759335]

Driedger PE, Blumberg PM. The effect of phorbol diesters on chicken embryo fibroblasts. Cancer Res. 1977; 37:3257–3265. [PubMed: 195722]

Edelstein, A.; Amodaj, N.; Hoover, K.; Vale, R.; Stuurman, N. Computer control of microscopes using microManager. In: Ausubel, Frederick M., et al., editors. Current protocols in molecular biology. 2010. Chapter 14, Unit14 20

Flier JS, Mueckler MM, Usher P, Lodish HF. Elevated levels of glucose transport and transporter messenger RNA are induced by ras or src oncogenes. Science. 1987; 235:1492–1495. [PubMed: 3103217]

Gibbs EM, Allard WJ, Lienhard GE. The glucose transporter in 3T3-L1 adipocytes is phosphorylated in response to phorbol ester but not in response to insulin. J Biol Chem. 1986; 261:16597–16603. [PubMed: 3536929]

Hresko RC, Kruse M, Strube M, Mueckler M. Topology of the Glut 1 glucose transporter deduced from glycosylation scanning mutagenesis. J Biol Chem. 1994; 269:20482–20488. [PubMed: 8051147]

Klepper J, Leiendecker B. Glut1 deficiency syndrome and novel ketogenic diets. Journal of child neurology. 2013; 28:1045–1048. [PubMed: 23666044]

Lee LS, Weinstein IB. Membrane effects of tumor promoters: stimulation of sugar uptake in mammalian cell cultures. J Cell Physiol. 1979; 99:451–460. [PubMed: 457799]

Leen WG, Klepper J, Verbeek MM, Leferink M, Hofste T, van Engelen BG, Wevers RA, Arthur T, Bahi-Buisson N, Ballhausen D, et al. Glucose transporter-1 deficiency syndrome: the expanding clinical and genetic spectrum of a treatable disorder. Brain. 2010; 133:655–670. [PubMed: 20129935]

Mann GE, Yudilevich DL, Sobrevia L. Regulation of amino acid and glucose transporters in endothelial and smooth muscle cells. Physiological reviews. 2003; 83:183–252. [PubMed: 12506130]

Miinea CP, Lienhard GE. Stoichiometry of site-specific protein phosphorylation estimated with phosphopeptide-specific antibodies. BioTechniques. 2003; 34:828–831. [PubMed: 12703308]

Mullen SA, Suls A, De Jonghe P, Berkovic SF, Scheffer IE. Absence epilepsies with widely variable onset are a key feature of familial GLUT1 deficiency. Neurology. 2010; 75:432–440. [PubMed: 20574033]

Nishikawa K, Toker A, Johannes FJ, Songyang Z, Cantley LC. Determination of the specific substrate sequence motifs of protein kinase C isozymes. J Biol Chem. 1997; 272:952–960. [PubMed: 8995387]

Nishimura H, Pallardo FV, Seidner GA, Vannucci S, Simpson IA, Birnbaum MJ. Kinetics of GLUT1 and GLUT4 glucose transporters expressed in Xenopus oocytes. J Biol Chem. 1993; 268:8514–8520. [PubMed: 8473295]

O'Brien TG. Hexose transport in undifferentiated and differentiated BALB/c 3T3 preadipose cells: effects 12-O-tetradecanoylphorbol-13-acetate and insulin. J Cell Physiol. 1982; 110:63–71. [PubMed: 7040424]

Seidner G, Alvarez MG, Yeh JI, O'Driscoll KR, Klepper J, Stump TS, Wang D, Spinner NB, Birnbaum MJ, De Vivo DC. GLUT-1 deficiency syndrome caused by haploinsufficiency of the blood-brain barrier hexose carrier. Nat Genet. 1998; 18:188–191. [PubMed: 9462754]

Sone H, Deo BK, Kumagai AK. Enhancement of glucose transport by vascular endothelial growth factor in retinal endothelial cells. Investigative ophthalmology & visual science. 2000; 41:1876–1884. [PubMed: 10845612]

Suls A, Mullen SA, Weber YG, Verhaert K, Ceulemans B, Guerrini R, Wuttke TV, Salvo-Vargas A, Deprez L, Claes LR, et al. Early-onset absence epilepsy caused by mutations in the glucose transporter GLUT1. Ann Neurol. 2009; 66:415–419. [PubMed: 19798636]

Tang W, Richards EM, Raizada MK, Sumners C. Angiotensin II increases glucose uptake and glucose transporter-1 mRNA levels in astroglia. The American journal of physiology. 1995; 268:E384–390. [PubMed: 7900784]

Vergarajauregui S, Oberdick R, Kiselyov K, Puertollano R. Mucolipin 1 channel activity is regulated by protein kinase A-mediated phosphorylation. Biochem J. 2008; 410:417–425. [PubMed: 17988215]

Wang D, Yang H, Shi L, Ma L, Fujii T, Engelstad K, Pascual JM, De Vivo DC. Functional studies of the T295M mutation causing Glut1 deficiency: glucose efflux preferentially affected by T295M. Pediatric research. 2008; 64:538–543. [PubMed: 18614966]

Weber YG, Storch A, Wuttke TV, Brockmann K, Kempfle J, Maljevic S, Margari L, Kamm C, Schneider SA, Huber SM, et al. GLUT1 mutations are a cause of paroxysmal exertion-induced dyskinesias and induce hemolytic anemia by a cation leak. J Clin Invest. 2008; 118:2157–2168. [PubMed: 18451999]

Wieman HL, Wofford JA, Rathmell JC. Cytokine stimulation promotes glucose uptake via phosphatidylinositol-3 kinase/Akt regulation of Glut1 activity and trafficking. Mol Biol Cell. 2007; 18:1437–1446. [PubMed: 17301289]

Witters LA, Vater CA, Lienhard GE. Phosphorylation of the glucose transporter in vitro and in vivo by protein kinase C. Nature. 1985; 315:777–778. [PubMed: 3159967]

Yamamoto T, Seino Y, Fukumoto H, Koh G, Yano H, Inagaki N, Yamada Y, Inoue K, Manabe T, Imura H. Over-expression of facilitative glucose transporter genes in human cancer. Biochem Biophys Res Commun. 1990; 170:223–230. [PubMed: 2372287]

Younes M, Lechago LV, Somoano JR, Mosharaf M, Lechago J. Wide expression of the human erythrocyte glucose transporter Glut1 in human cancers. Cancer Res. 1996; 56:1164–1167. [PubMed: 8640778]

Highlights

- PKC phosphorylates GLUT1 on S226 *in vitro* and *in vivo* in endothelial cells
- TPA induces rapid increases in glucose uptake require S226 phosphorylation
- Phosphorylation of S226 increases GLUT1 membrane localization
- Some GLUT1 deficiency syndrome mutations show impaired S226 phosphorylation

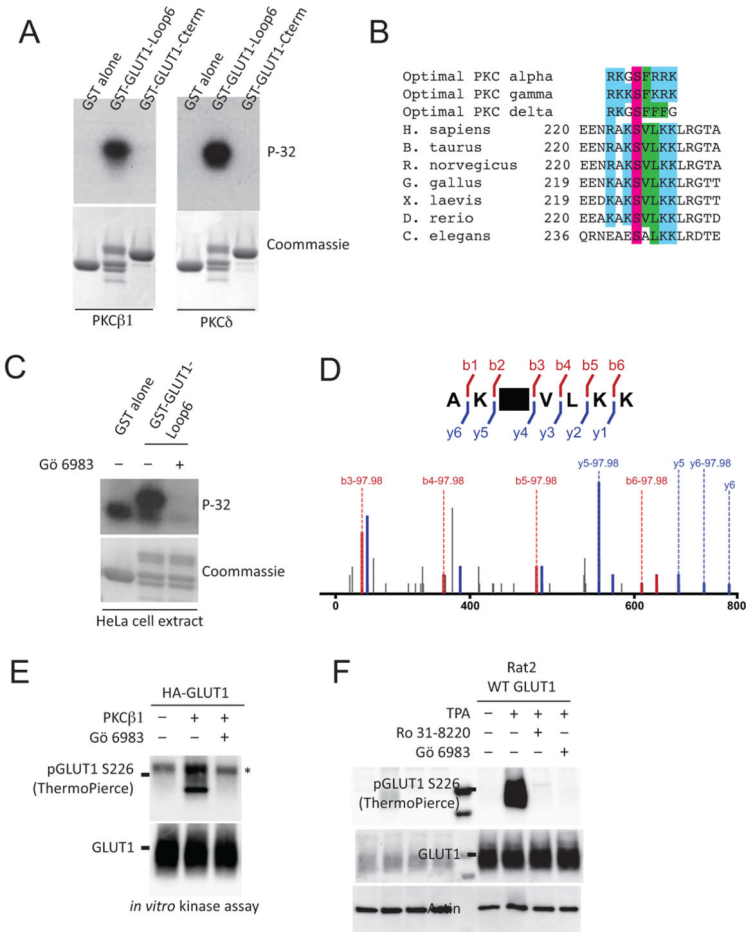

Figure 1.

GLUT1 is phosphorylated *in vivo* and *in vitro*. A) The central cytoplasmic loop of GLUT1 (Loop 6) is phosphorylated by PKCβ1 and PKCδ *in vitro*. B) Sequence of vertebrate homologs of GLUT1 show conservation of several residues surrounding S226 when compared to optimal PKC consensus phosphorylation motifs. Colors (blue, basic; purple, serine; green, hydrophobic) highlight conserved residues. C) HeLa cell extract phosphorylates GST-GLUT1-Loop6 but this phosphorylation can be efficiently inhibited by a PKC inhibitor (Gö-6983). D) HA-GLUT1 purified from TPA-treated Rat2 fibroblasts were trypsin digested and analyzed by Q-exactive mass spectrometry. Labeled N-terminal (red) and C-terminal (blue) peaks unambiguously confirm phosphorylation of S226. Many peptides show neutral loss of phosphoric acid (−97.98/z), which is also consistent with phosphorylation at S226. E) PKCβ1 phosphorylates full length HA-GLUT1 *in vitro* but not in the presence of Gö-6983. Asterisk indicates a non-specific band. F) Phosphorylation of WT GLUT1 is induced by TPA and inhibited by PKC inhibitors, Rö-31-8220 and Gö-6983. The pGLUT1 S226 blot was stripped and reprobed for Actin. See also Figure S1, S2, and Table S1.

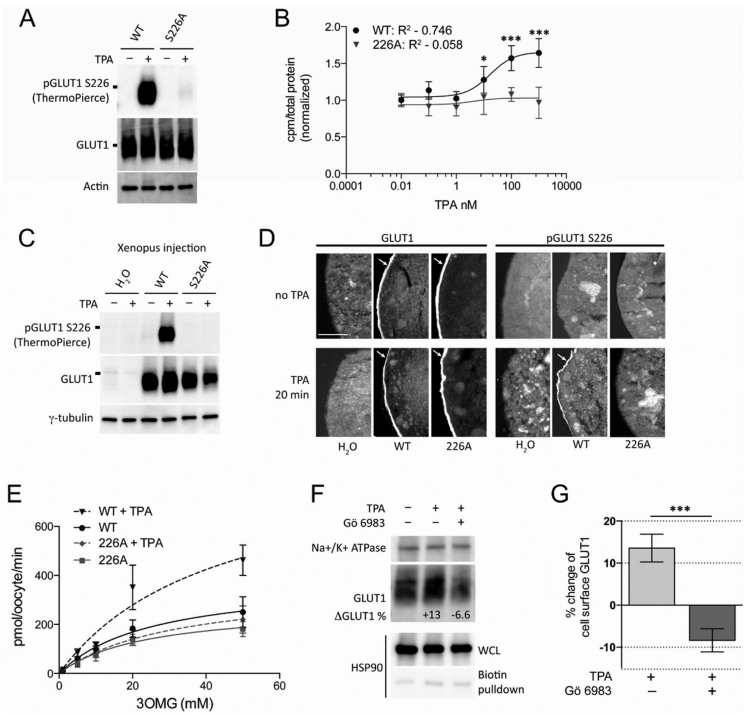

Figure 2.

GLUT1 S226A is impaired in its response to TPA. A) WT, but not S226A, GLUT1 is specifically phosphorylated on S226 after treatment with TPA in Rat2 cells. pGLUT1 S226 blot was stripped and reprobed for Actin. B) Rat2 fibroblasts expressing WT, but not S226A, GLUT1 increase 2DG uptake within 30 minutes of treatment by TPA. Data fit against a three parameter dose response curve. (n=6 independent experiments, each performed in triplicate, error bars = SD). C) Western blot from membranes of 10 oocytes injected with the indicated *in vitro* transcribed mRNA or water (2 days) followed by treatment with TPA (20 min) demonstrates that the WT GLUT1 is phosphorylated after TPA treatment. D) Immunoflourescent images from oocytes injected with the indicated mRNA (bottom) followed by staining with the indicated antibody (top) with or without TPA treatment demonstrate comparable expression and trafficking of WT and 226A transporter to the cell membrane. Phosphorylated GLUT1 is only detected after TPA treatment of WT GLUT1. Bar = 100μm. Arrow indicates membrane staining. E) TPA treatment markedly increases 3-OMG uptake by WT but not 226A mutant transporters (n=10, error bars = SEM) in oocytes. F) Biotin pulldown of surface proteins demonstrates that endogenous GLUT1 increases its membrane (normalized against Na+/K+ ATPase) abundance after treatment with TPA in Rat2 cells; this is blocked by pre-treatment with a PKC inhibitor. HSP90 blot demonstrates the decrease in cytoplasmic protein concentration after biotin pulldown for membrane proteins. G) Quantitation of biotin pulldown experiments demonstrates significant increase in membrane GLUT1 induced by TPA (n=4, error bars = SEM). t-test, *p<0.05, **p<0.01, ***p<0.001. See also Figure S3.

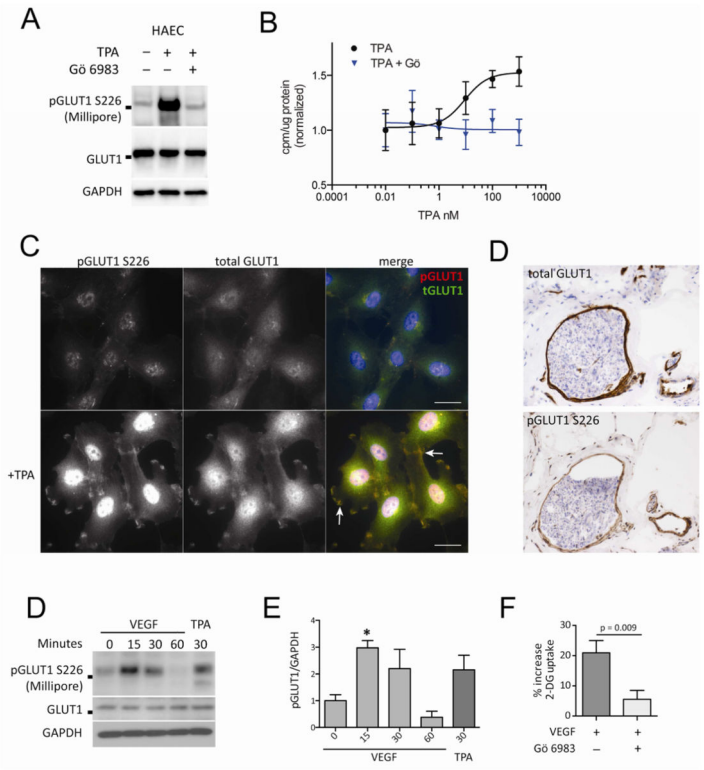

Figure 3.

Phosphorylation and localization of GLUT1 in primary endothelial cells. A) Endogenouse GLUT1 in human aortic endothelial cells (HAEC) is phosphorylated on S226 in response to TPA; the phosphorylation is blocked by a PKC inhibitor. B) HAEC increases 2DG uptake within 30 minutes of treatment by TPA. This increase is blocked by pretreatment with Gö-6983 (n=3, error bars = SD). C) Human umbilical vein endothelial cells (HUVEC) stained with DAPI (blue), total GLUT1 (green), and pGLUT1 S226 (red). Membrane staining of total GLUT1 (middle column) is apparent after TPA stimulation (bottom row). pGLUT1 (left column) shows a striking increase after TPA treatment with clear localization to cell membranes after TPA treatment. Arrows highlight regions of GLUT1 and pGLUT1 colocalization at membrane ruffles. Bar=25μm D) Total GLUT1 and pGLUT1 S226 staining in consecutive frozen sections from a patient biopsy sample (lymphatic malformation) showing partial overlap of GLUT1 and pGLUT1 staining. Both antibodies stain the perineurium as demonstrated by the rim of staining around the large peripheral nerve. E) HUVECs phosphorylate endogenous GLUT1 in response to GLUT1 in response to VEGF (100ng/ml) in a time dependent manner. F) Quantitation of pGLUT1 normalized to GAPDH showed significant differences in phosphorylation of GLUT1 in response to VEGF (n=5, error bars = SEM; ANOVA, p=0.004; Tukey's, $p<0.05$). G) VEGF rapidly increase 2-DG uptake in response to VEGF (100ng/ml). This increase inhibited by pretreatment with pretreatment with Gö-6983 (n=3, error bars = SEM, t-test). See also Figure S4.

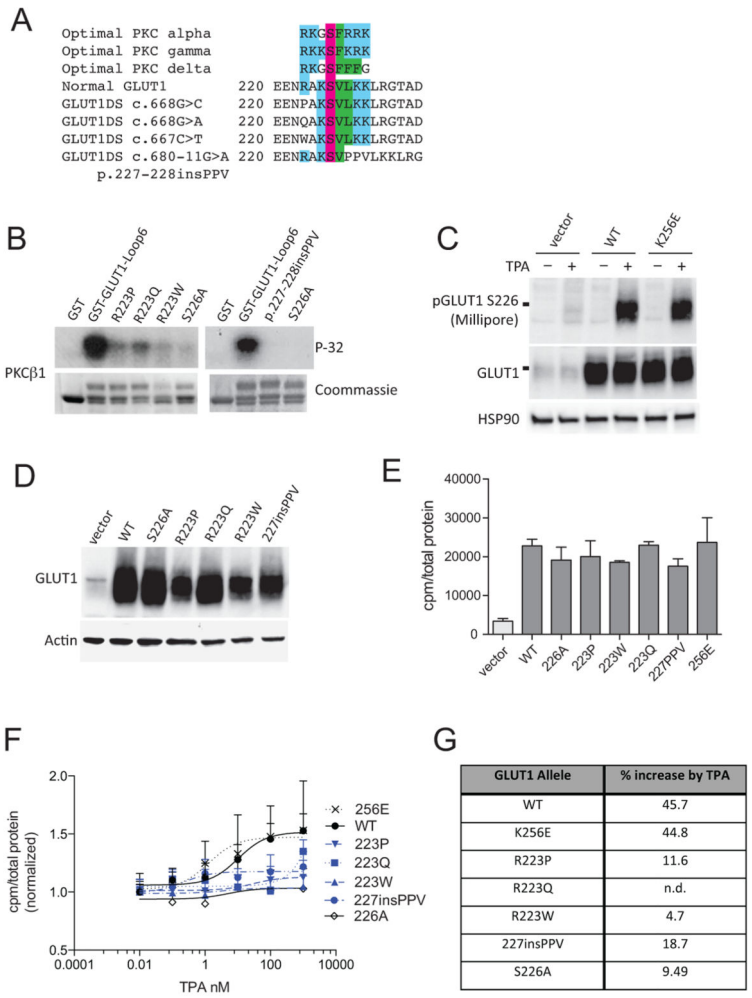

Figure 4.

G1D mutations inhibit S226 phosphorylation and response to TPA. A) Sequence alignment of patient derived G1D mutations that highlight the loss of conserved residues of the optimal PKC consensus motifs. B) Patient derived G1D mutations surrounding the S226 motif decrease the ability of PKCβ1 to phosphorylate GST-GLUT1-Loop6 *in vitro*. Autoradiogram and Coommassie are representative of ≥3 independent experiments. C) Compared to WT GLUT1, K256E is stably expressed and shows comparable levels of phosphorylation after treatment with TPA. D) WT, R223P, R223Q, R223W, and 227insPPV are stably expressed in Rat2 fibroblasts. E) No significant difference between basal 2-DG uptake by WT compared to 226A, 223P, 223Q, 223W, 223Q, 227inPPV, or 256E mutant transporters (n≥3, error bars = SEM; Dunnett's). F) 2-DG uptake by R223P, R223Q, R223W, and 227insPPV are impaired in their response to TPA [(n≥3, except K256E, n=2)]. G) Maximal TPA-induced increases in glucose uptake are impaired in naturally-occurring, pathogenic mutations surrounding S226.